

PAPER • OPEN ACCESS

# Gravitational wave signals from leptoquark-induced first-order electroweak phase transitions

To cite this article: B. Fu and S.F. King JCAP05(2023)055

View the [article online](#) for updates and enhancements.

You may also like

- [Leptoquark single and pair production at LHC with CalcHEP/CompHEP in the complete model](#)  
Alexander Belyaev, Claude Leroy, Rashid Mehdiyev et al.
- [Leptoquark production at LHC](#)  
Ajla Lejli
- [Collider signature of  \$U\$ , Leptoquark and constraints from  \$b\$   \$c\$  observables](#)  
Aritra Biswas, Dilip Kumar Ghosh, Nivedita Ghosh et al.

# Gravitational wave signals from leptoquark-induced first-order electroweak phase transitions

B. Fu  and S.F. King 

Department of Physics and Astronomy, University of Southampton,  
SO17 1BJ Southampton, United Kingdom

E-mail: [B.Fu@soton.ac.uk](mailto:B.Fu@soton.ac.uk), [king@soton.ac.uk](mailto:king@soton.ac.uk)

Received November 14, 2022

Revised March 7, 2023

Accepted April 14, 2023

Published May 26, 2023

**Abstract.** We consider the extension of the Standard Model (SM) with scalar leptoquarks in SU(2) singlet, doublet and triplet representations. Through the coupling between leptoquark and the SM Higgs field, the electroweak phase transition (EWPT) can turn into first-order and consequently produce gravitational wave signals. We compute the required value of the leptoquark-Higgs for first-order EWPT to happen and discuss about the possible constraint from Higgs phenomenology. Choosing some benchmarks, we present the strength of the gravitational waves produced during the leptoquark-induced first-order EWPT and compare them to detector sensitivities. We find that the SU(2) representations of the leptoquark can be distinguished by gravitational waves in the parameter space where first-order EWPT can happen as a function of the Higgs portal coupling.

**Keywords:** cosmology of theories beyond the SM, particle physics - cosmology connection

**ArXiv ePrint:** [2209.14605](https://arxiv.org/abs/2209.14605)



---

## Contents

<b>1</b>	<b>Introduction</b>	<b>1</b>
<b>2</b>	<b>First-order EWPT induced by scalar leptoquarks</b>	<b>2</b>
2.1	Constraints on the Higgs portal coupling	6
<b>3</b>	<b>Gravitational wave signals</b>	<b>7</b>
<b>4</b>	<b>Conclusion</b>	<b>10</b>
<b>A</b>	<b>Production of gravitational waves during a first-order phase transition</b>	<b>11</b>

---

## 1 Introduction

Leptoquarks (LQs) are hypothetical particles that can convert quarks into leptons and vice versa with great interest in elementary particle physics. From the theoretical aspect, it has been predicted naturally by the Pati-Salam unification of quarks and leptons [1, 2], where the leptoquark is first raised, as well as many other grand unified theories [3–9]. From the experimental side, the existence of leptoquarks is strongly indicated by lepton flavour universality violation (LFUV) in semi-leptonic  $B$  decay [10–15]. Besides LFUV, leptoquarks can also be related to a wide variety of phenomena beyond the standard model, including the muon  $g - 2$  [16–21], the neutrino mass [22–26] and the  $W$  boson mass [27–32].

Despite the theoretical and experimental attraction from leptoquarks, they have not been found by any collider experiment so far. One of the possibilities to find leptoquark is through its connection to Higgs phenomenology [33, 34]. Generically, the scalar leptoquarks can couple to Higgs boson in the scalar potential. After electroweak symmetry breaking, the leptoquark-Higgs operator induces the couplings to the physical Higgs boson, which can further affect loop-induced Higgs production and decay processes. Such effects can be probed with the Higgs signal strength measurements at colliders and thus are potential smoking guns for leptoquarks.

In the meantime, the Higgs portal allows leptoquarks to modify the EWPT in the early universe. It has been shown that first-order EWPT can be induced by an additional singlet scalar field without any vacuum expectation value (VEV) [35]. And the stochastic gravitational wave background produced during the cosmological phase transition can be potentially tested by detectors [36–38]. This provides us with a new possibility of testing scalar leptoquarks, using a similar approach to the singlet, from cosmic signals.

In this paper, we extend the study of first-order EWPT induced by an extra singlet scalar to the case of scalar leptoquarks in  $SU(2)$  singlet, doublet and triplet representations, and show how such leptoquarks can affect the EWPT through their coupling to the standard model Higgs boson. By computing the effective scalar potential, we find the range of Higgs portal coupling where eligible first-order EWPT can happen for different types of scalar leptoquark with a mass around TeV scale. Then we apply the standard procedure [39–47] to calculate the gravitational wave background produced during the first-order EWPT induced by leptoquark for some benchmark cases and compare it with the detector sensitivities. We

found that in some range of the parameter space, the leptoquark-induced first-order EWPT is able to produce gravitational wave signals that are strong enough to be detected.

The paper is organised as follows. In section 2, we discuss the first-order EWPT induced by leptoquark through the Higgs portal. We also show the constraints from Higgs physics to the parameter space. In section 3, we show the gravitation wave signal produced during leptoquark-induced first-order EWPT for benchmark points. Finally, we summarise and conclude in section 4.

## 2 First-order EWPT induced by scalar leptoquarks

In this section, we discuss how a first-order EWPT can be induced by leptoquarks. We consider the coupling between the SM scalar doublet  $H$  and an extra complex scalar leptoquark  $S$  with a SU(2) index  $a$ , which runs up to 1, 2 or 3 for singlet, doublet or triplet representations, respectively. In the simplest case, the scalar potential can be written as

$$V_0 = -\mu^2|H|^2 + \lambda_H|H|^4 + \mu_S^2|S_a|^2 + \lambda_S|S_a|^4 + 2\lambda_{HS}|H|^2|S_a|^2 \quad (2.1)$$

For simplicity, we only consider the minimal quartic interaction between Higgs and scalar leptoquark in the form of  $|H|^2|S|^2$ . Other forms of quartic interactions, such as  $|H^\dagger S|^2$  for SU(2) doublet leptoquark and  $H^\dagger(\sigma^i S_i)(\sigma^j S_j)^\dagger H$  for SU(2) triplet leptoquark, can lead to mass shifts between the SU(2) components of leptoquarks after spontaneous symmetry breaking (SSB), as well as extra contributions to the thermal mass of the SM Higgs field. Such contributions can enhance the phase transition, but the effect can be taken into account effectively by shifting the minimal quartic coupling  $\lambda_{HS}$ . Focussing on the field  $h$  in  $H = (G^+, (h + iG^0)/\sqrt{2})$  that becomes the SM Higgs boson after spontaneous symmetry breaking, the scalar potential reads

$$V_0 = -\frac{\mu^2}{2}h^2 + \frac{\lambda_H}{4}h^4 + \frac{\mu_S^2}{2}(s_{a,1}^2 + s_{a,2}^2) + \frac{\lambda_S}{4}(s_{a,1}^2 + s_{a,2}^2)^2 + \frac{\lambda_{HS}}{2}h^2(s_{a,1}^2 + s_{a,2}^2) \quad (2.2)$$

where  $S_a = (s_{a,1} + i s_{a,2})/\sqrt{2}$ . As the leptoquark is typically heavier than the electroweak scale, we assume  $\mu_S^2 > 0$  in this research. Then the leptoquark mass after SSB is  $m_S^2 = \mu_S^2 + \lambda_{HS}v_0^2$  with  $v_0$  the standard model Higgs VEV. At tree level, the phase transition is second-order as the participation of  $S$  does not vary the minimum of the scalar potential. However, by considering the finite temperature effective potential, the existence of leptoquarks modifies the minimum through the Higgs portal coupling at loop order. In this study, we consider the effective potential at one-loop level for simplicity, neglecting higher-order effects [48] that may vary the transition strength by 20%. We also neglect renormalisation group corrections which have a smaller effect [49].

At one-loop level, the effective scalar potential receives contributions from zero-temperature correction  $\Delta V_0^{1\text{-loop}}$  (Coleman-Weinberg potential) and finite-temperature correction  $\Delta V_T^{1\text{-loop}}$  [50]

$$V_{\text{eff}}(h, T) = V_0 + \Delta V_0^{1\text{-loop}}(h) + \Delta V_T^{1\text{-loop}}(h, T). \quad (2.3)$$

The one-loop zero-temperature correction reads

$$\Delta V_0^{1\text{-loop}}(h) = \sum_{i \in b, f} \frac{n_i}{64\pi^2} \left[ m_i^4(h) \left( \ln \frac{m_i^2(h)}{m_i^2(v_0)} - \frac{3}{2} \right) + 2m_i^2(h)m_i^2(v_0) \right], \quad (2.4)$$

where  $m_i^2 = m_{0i}^2 + a_i h^2$  are the shifted masses with

$$m_{0\{t,W,Z,h,G,S\}}^2 = \{0, 0, 0, -\mu^2, -\mu^2, \mu_S^2\}, \quad (2.5a)$$

$$a_{\{t,W,Z,h,G,S\}} = \left\{ \frac{y_t^2}{2}, \frac{g^2}{4}, \frac{g^2 + g'^2}{4}, 3\lambda_H, \lambda_H, \lambda_{HS} \right\}, \quad (2.5b)$$

$$n_{\{t,W,Z,h,G,S\}} = \{-12, 6, 3, 1, 3, n_S\}. \quad (2.5c)$$

The quantity  $v_0$  is the SM Higgs VEV at zero temperature. The degree of freedom  $n_S$  in the complex SU(3) triplet  $S$ , depending on the SU(2) representation of the leptoquark, can be 6 for SU(2) singlet, 12 for SU(2) doublet or 18 for SU(2) triplet.

The one-loop finite-temperature correction in eq. (2.3) is

$$\Delta V_T^{1\text{-loop}}(h, T) = \sum_{i \in b} \frac{n_i T^4}{2\pi^2} J_b \left( \frac{m_i^2}{T^2} \right) + \sum_{i \in f} \frac{n_i T^4}{2\pi^2} J_f \left( \frac{m_i^2}{T^2} \right) \quad (2.6)$$

where  $b$  and  $f$  stand for bosons and fermions and

$$J_{b/f} \left( \frac{m_i^2}{T^2} \right) = \int_0^\infty dx x^2 \ln \left[ 1 \mp e^{-\sqrt{x^2 + m_i^2(h)/T^2}} \right]. \quad (2.7)$$

At high temperature  $T \gtrsim m_i$ ,  $J_b$  and  $J_f$  can be expanded as

$$J_b \left( \frac{m_i^2}{T^2} \right) \simeq -\frac{\pi^4}{45} + \frac{\pi^2 m_i^2}{12 T^2} - \frac{\pi m_i^3}{6 T^3} - \frac{1}{32} \frac{m_i^4}{T^4} \left( \ln \frac{m_i^2}{T^2} - c_b \right) + \dots \quad (2.8a)$$

$$J_f \left( \frac{m_i^2}{T^2} \right) \simeq \frac{7\pi^4}{360} - \frac{\pi^2 m_i^2}{24 T^2} - \frac{1}{32} \frac{m_i^4}{T^4} \left( \ln \frac{m_i^2}{T^2} - c_f \right) + \dots \quad (2.8b)$$

with  $c_b \simeq 5.4$  and  $c_f \simeq 2.6$ . At low temperature  $T < m_i$ ,  $J_b$  is exponentially suppressed as its argument increases.

The inclusion of Goldstone degrees of freedom in eq. (2.4) leads to an infrared logarithmic divergence as the Goldstone bosons are massless at the zero-temperature vacuum. Such a problem is also related to the perturbativity of couplings at high temperature [51] and can be solved by resumming the ring (daisy) diagrams [50, 52]. There are two different methods that are widely used for resummation. In the Parwani method [53], the shifted masses of scalars and the longitudinal models of the gauge bosons in the effective potential are replaced by the Debye masses  $M_i^2(h, T) = m_i^2(h) + \Pi_i(T)$ , where the self-energies  $\Pi_i(T)$  are given by  $\Pi_i(T) = b_i T^2$  with [54]

$$b_h = b_G = \frac{3g^2 + g'^2}{16} + \frac{\lambda_H}{2} + \frac{y_t^2}{4} + \frac{n_S \lambda_{HS}}{12}, \quad b_W = b_Z(T) = \frac{11}{6} g^2, \quad b_\gamma = \frac{11}{6} g'^2, \\ b_S = \begin{cases} \frac{\lambda_{HS}}{3} + \frac{(n_S + 2)\lambda_S}{12} + \frac{3}{4} g_3^2 + \frac{1}{4} Y^2 + \frac{g'^2}{16} & \text{SU(2) singlet,} \\ \frac{\lambda_{HS}}{3} + \frac{(n_S + 2)\lambda_S}{12} + \frac{3}{4} g_3^2 + \frac{1}{4} Y^2 + \frac{3g^2 + g'^2}{16} & \text{SU(2) doublet and triplet.} \end{cases} \quad (2.9)$$

In the Arnold-Espinosa method [55], the replacement only happens in the mass cubic terms. While the Arnold-Espinosa resummation avoids some unphysical linear terms that shift the

symmetric minimum away from the origin, it fails at low temperatures as the method relies on the expansion in eq. (2.8a). In this paper, we adapt the Parwani method in order to achieve a smooth connection to correct low-temperature thermal correction [52, 56]. While the leptoquark coupling  $Y$  is typically smaller than the unitarity [57], the SU(3) coupling can have significant contribution to the Debye mass of the leptoquarks. However, the contributions, not only from the SU(3) coupling but also from other gauge couplings, play the same role as the one from self-interaction coupling  $\lambda_S$  in the phase transition and thus can be absorbed effectively by shifting  $\lambda_S$  to  $\tilde{\lambda}_S$ . This kind of shift can change the parameter space where first-order phase transition can happen. However, as  $\lambda_S$  is unconstrained, the discussion on the effect of  $\tilde{\lambda}_S$  is less meaningful unless when  $\lambda_S$  approaches its perturbativity limit. Therefore we focus on the effect of varying the Higgs portal coupling  $\lambda_{HS}$  and fix the value of  $\tilde{\lambda}_S$  as in [35, 39]. Considering the contributions from the gauge couplings and leptoquark-fermion couplings, we fix  $\tilde{\lambda}_S$  to be 2.

When the phase transition happens at a low temperature, the effective potential can develop an imaginary part as the thermal masses of Goldstone bosons become negative. It has been pointed out in [58] that such an imaginary part remarks the decay rate of the quantum state minimising the Hamiltonian.

In the simplest case, the *sufficient*<sup>1</sup> conditions for an “eligible” first-order EWPT to occur are

1. The electroweak minimum is the true minimum at zero temperature  $T = 0$  and  $h = 0$  is a local maximum ( $V''(0, 0) < 0$ ).
2. At the temperature  $T_2$  that  $h = 0$  change from a local maximum to a local minimum, there is another non-zero local minimum.

The first condition ensures that the phase transition is completed today. If  $h = 0$  is a local minimum at zero temperature, the phase transition can only happen through tunnelling and the probability is too low to finish the transition to the true vacuum today. The second condition ensures that there are two minima existing simultaneously during the phase transition. In a scenario satisfying both conditions, the two minima of the scalar potential are degenerate at a critical temperature  $T_c$ . The allowed parameter spaces for first-order phase transition to happen are shown as the coloured regions in figure 1. The strength of the transition can be estimated by the ratio of the non-zero VEV and the critical temperature,  $v_c/T_c$ , which is shown as the colour in figure 1. Above the coloured regions, the first-order EWPT is not eligible as condition 1 is not satisfied; below the coloured regions, first-order EWPT cannot happen because condition 2 is not satisfied.

In figure 1(a) to figure 1(c), the required coupling for first-order EWPT increases as the leptoquark becomes heavier in each SU(2) representation of leptoquark. By comparing different panels and also by comparing the lines with different colours in figure 1(d), it can be figured out that the Higgs portal coupling required for first-order EWPT becomes smaller as the dimension of the leptoquark SU(2) representation increases. Empirical expressions of the interesting parameter spaces can be obtained when the leptoquark is heavy. For leptoquark mass above 1 TeV, the allowed Higgs portal for eligible first-order EWPT to happen is roughly between

---

<sup>1</sup>First-order phase transitions can happen even if the conditions listed below are not satisfied. An example is the green region in figure 1(d). However, we expect the strength of first order phase transition to be relatively weak in that region and unlikely to produce detectable gravitational waves. For simplicity, we only consider first-order phase transitions satisfying the conditions below.

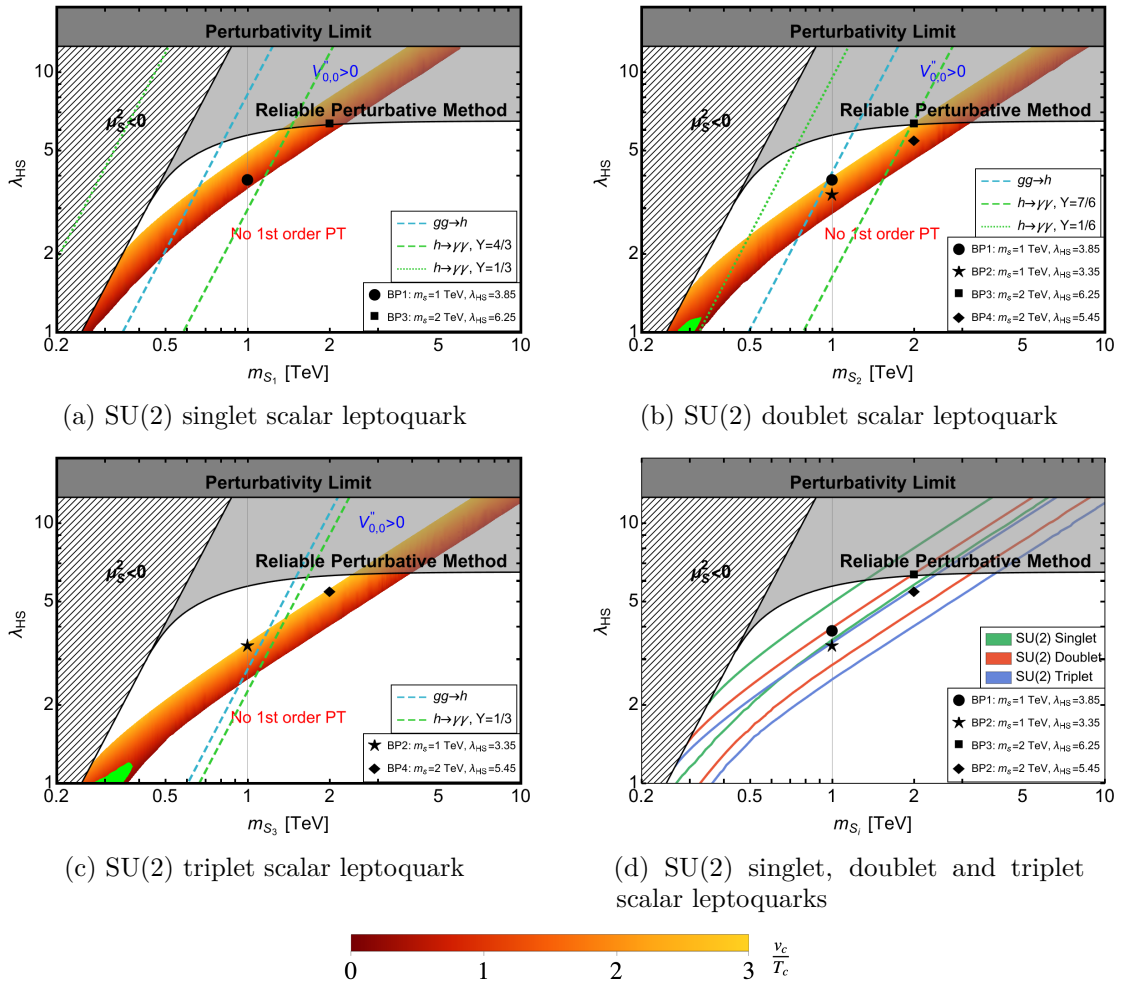


**Figure 1.** Allowed parameter space for first-order phase transition induced by different types of scalar leptoquark. Detailed discussion can be found in the text.

$\{3.59, 4.99\} \times (m_{S_1}/1 \text{ TeV})^{0.685}$  for singlet leptoquark, between  $\{2.87, 4.00\} \times (m_{S_2}/1 \text{ TeV})^{0.679}$  for doublet leptoquark and between  $\{2.52, 3.50\} \times (m_{S_3}/1 \text{ TeV})^{0.676}$  for triplet leptoquark.

A more complicated case can occur when the scalar potential develops two non-zero minima simultaneously after the temperature drops below  $T_2$ . In such a case, the transition has two steps: first to a non-zero minimum continuously through second-order phase transition and then to the larger non-zero minimum through first-order phase transition. The regions where such cases happen are marked as green in figure 1(b) and figure 1(c). However, as the leptoquark is typically above 1 TeV, such regions are not of interest in this study.

Since the coupling that is required for a first-order phase transition to appear grows as the scalar mass increases, the perturbative method used in the effective potential calculation can break down. To estimate the reliability of the perturbative method, we evaluate the loop contribution to the Higgs quartic coupling as has been done in [35]. Since the main concern is the Higgs portal coupling  $\lambda_{HS}$ , we consider the higher loop contributions from the leptoquarks only involving Higgs portal vertices. Although the contribution to the Higgs quartic coupling from the leptoquarks is proportional to its internal degrees of freedom, the

leptoquarks with different quantum numbers contribute separately as only the Higgs portal vertices are considered. Therefore, the ratio between the one-loop and two-loop corrections is independent of the leptoquark internal degrees of freedom and can be estimated as the one-loop correction from each leptoquark component

$$\frac{\delta\lambda_H^{2\text{-loop}}}{\delta\lambda_H^{1\text{-loop}}} \sim \frac{\lambda_{HS}}{16\pi^2} \left( \ln \frac{\mu_S^2 + \Lambda_{HS} h^2}{m_S^2} - \frac{3}{2} \right). \quad (2.10)$$

To ensure the reliability of the perturbative method, we choose 0.2 to be the approximate threshold for the ratio above. In figure 1, the region where the perturbative method is no longer reliable is marked out by the shadows area.

## 2.1 Constraints on the Higgs portal coupling

The new interaction between a scalar leptoquark and the Higgs doublet can affect the Higgs boson production and decay processes. The discrepancy between SM prediction and experimental measurement is commonly characterised by the  $\varkappa$ -factor, defined as  $\varkappa_i = \sqrt{\Gamma_i^{\text{exp}}/\Gamma_i^{\text{SM}}}$  [59, 60]. The loop-induced contribution from leptoquark to the Higgs boson decay process into photons and the gluon-gluon production of Higgs boson are given by [34]

$$\varkappa_g = 1 + 0.24 \frac{\lambda_{HS} v^2}{m_S^2} N_S \quad (2.11)$$

$$\varkappa_\gamma = 1 - 0.052 \frac{\lambda_{HS} v^2}{m_S^2} N_c \sum_i Q_i^2 \quad (2.12)$$

where the sum is taken over all SU(2) components of the leptoquark and  $Q_i$  is the electric charge of the  $i$ th component.  $N_S$  is the number of the leptoquark SU(2) components. The experimental measurements by the ATLAS collaboration are  $\varkappa_g = 1.01_{-0.09}^{+0.11}$  and  $\varkappa_\gamma = 1.02_{-0.07}^{+0.08}$  [61]. Similar contribution appears in the decay channel of Higgs into a  $Z$  boson and a photon as well, in the form of [34]

$$\varkappa_{Z\gamma} = 1 + 0.036 \frac{\lambda_{HS} v^2}{m_S^2} N_c \sum_i Q_i \left( I_i^W - 0.23Q_i \right) \quad (2.13)$$

where  $I_i^W$  is the value of the weak isospin of the leptoquark. The value of  $\varkappa_{Z\gamma}$  measured by CMS collaboration is  $1.65_{-0.37}^{+0.34}$  [62]. Despite abundant collider phenomena caused by the Higgs portal to leptoquarks, none of the observables can constrain the portal coupling restrictedly. When multiple leptoquarks appear in a model, the contributions from different types of leptoquarks can have opposite contributions to the  $\varkappa$  parameters above. In order to visualise the effects of these observables, we consider the collider constraints under the assumption of a single leptoquark multiplet and show the maximal values of the Higgs portal allowed by  $h \rightarrow \gamma\gamma$  and  $gg \rightarrow h$  as the dashed and dotted lines in figure 1(a) to figure 1(c). While the  $gg \rightarrow h$  cross section is affected by the SU(2) representation of the leptoquark, the  $h \rightarrow \gamma\gamma$  cross section depends on the electric charge. For scalar leptoquark, assuming direct interaction to SM fermions, there are two different possible assignments of hypercharge for SU(2) singlet and doublet and one assignment for SU(2) triplet [63]: 4/3 or 1/3 for singlet, 7/6 or 1/6 for doublet and 1/3 for triplet. Although those constraints are currently weak, they are expected to be improved foreseeably by future experiments like HL-LHC [64], FCC [65, 66], ILC [67] and CEPC [68, 69]. Moreover, the Higgs portal coupling also affects flavour violating processes like the  $h \rightarrow \mu\tau$  or  $\tau \rightarrow \mu\gamma$  decay which can be tested by precious measurements at colliders [34, 70].



### 3 Gravitational wave signals

During a first-order phase transition, the scalar field configuration tunnels from the zero vacuum to a non-zero vacuum locally in the form of bubbles. The scalar bubbles can then move, collide and expand. Sound waves and turbulence can be produced after the collision of bubbles. The gravitational wave can be produced through three different mechanisms [36, 37]: *collision* between the scalar bubbles, overlap of the *sound wave* in the plasma and the fluid *turbulence*. The total gravitational wave spectrum is the sum of the three contributions

$$\Omega_{\text{tot}}(f) = \Omega_{\text{coll}}(f) + \Omega_{\text{sw}}(f) + \Omega_{\text{turb}}(f). \quad (3.1)$$

All three contributions depend on the phase transition dynamics which is described by four key parameters: the wall velocity  $v_w$ , the inverse phase transition duration  $\beta/\mathcal{H}_*$ , the phase transition strength  $\alpha_{T_*}$  and the transition temperature  $T_*$ . After these parameters are determined, the gravitational wave spectrum can be computed using results from numerical simulations.

The crucial step in computing these key parameters is to compute the Euclidean action. To find the Euclidean action which is defined as the spacial integration of the effective Lagrangian, a solution of the Euclidean equation of motion is required, which is generally not solvable analytically. For further details see appendix A. A common treatment for particles of electroweak scale or below is to make an approximation using eq. (2.8a) and eq. (2.8b) after which the effective potential can be simplified into a quartic function of the scalar field and a semi-analytical expression for the Euclidean action can be derived [40, 71]. However, as the leptoquark is typically above TeV scale [72–75], the one-loop finite-temperature correction from leptoquark is exponentially suppressed and thus negligible. On the other hand, the approximation in eq. (2.8a) and eq. (2.8b) are no longer eligible in the parameter space of interest. Therefore the Euclidean equation of motion is solved numerically in this work.

In figure 2 and figure 3, we show the gravitational wave produced from first-order EWPT for the 4 benchmark cases in figure 1. The cases with 1 TeV leptoquarks are shown in figure 2 and those with 10 TeV leptoquarks are shown in figure 3. In order to compare the result with detections, we shadow the region that can be detected by BBO [76], DECIGO [77, 78], LISA [36] and  $\mu$ Ares [79] with different colours. The gravitational waves produced by different sources during the phase transition are also shown independently. As the average bubble radius  $R_*$  at the percolation temperature is much larger than the initial bubble radius  $R_0$ , the gravitational wave produced by bubble collision is subdominant and can be neglected. We have also found that, for all the cases, the gravitational wave is dominantly produced by the turbulence at most frequencies, except around the peak frequency for the gravitational wave produced by the sound wave. The reason is that the sound wave period  $\tau_{sw}$  is relatively small compared with the Hubble time, which means more energy budget in the fluid motion is released in the form of turbulence than the sound wave. However, the calculation of gravitational wave from turbulence after a phase transition has a relatively large uncertainty, and the assumption of full conversion of the fluid motion energy into turbulence can also lead to an overestimation of the gravitational wave strength. Therefore the contribution from turbulence is shown as a reference on its upper bound. As the gravitational wave produced by sound wave dominates when it peaks, the sensitivity to Higgs portal coupling is not affected.

By comparing the panels, it can be noticed that the gravitational wave produced from first-order EWPT relies on the strength of the transition. To illustrate the relation more explicitly, we show the dependence of gravitational wave signal peak values on the strength

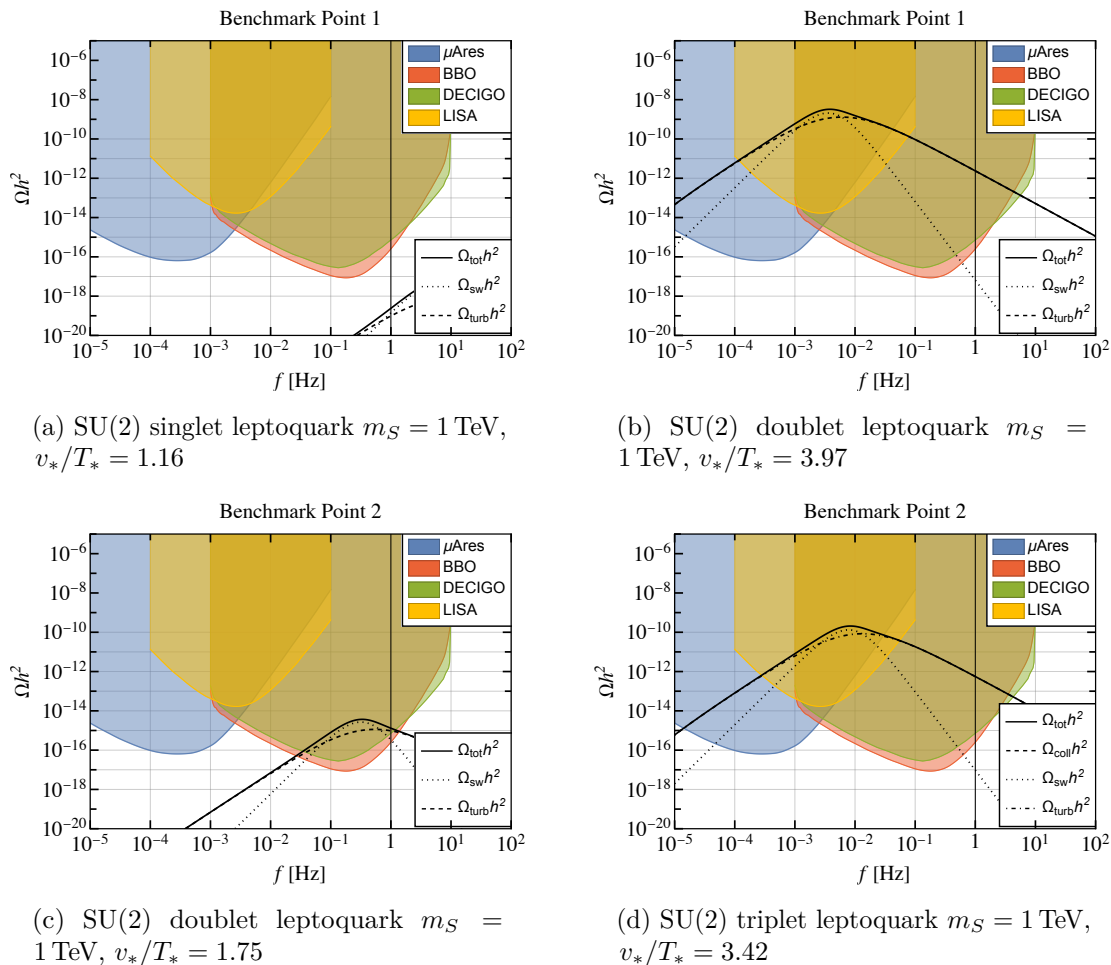


**Figure 2.** Gravitational wave signals for benchmark cases with 1 TeV leptoquarks. See the text for further discussion and explanation.

of the phase transition in the left panel of figure 4. Here, instead of  $v_c/T_c$  in the previous section, the strength of transition is estimated by the ratio of the non-zero minimum of the scalar potential and temperature when the phase transition happens, i.e. when the probability of bubble nucleation is significant. The temperature  $T_*$  is defined by the temperature when one bubble is nucleated per unit volume per unit time and the non-zero VEV at  $T_*$  is denoted as  $v_*$ . We find that the gravitational wave is testable when  $v_*/T_*$  is roughly larger than 1.22. In the right panel of figure 4, we show how the gravitational wave signal peak values rely on the Higgs portal coupling when the masses of leptoquarks are 1 TeV. For the first-order phase transitions induced by different types of leptoquarks, the gravitation wave signals achieve the same peak value when the Higgs portal couplings are in different ranges. The dashed and dot-dashed lines corresponds to the benchmark cases 1 and 2, respectively.

For the same benchmark point, the gravitational wave produced during first-order EWPT induced by leptoquark with a smaller intrinsic degree of freedom is stronger. In both figure 2 and figure 3, (a) and (b) show the result for the same benchmark point but in the case of singlet and doublet leptoquark, respectively, while (c) and (d) show the result for the same benchmark point but in the case of singlet and doublet leptoquark, respectively. It is clear

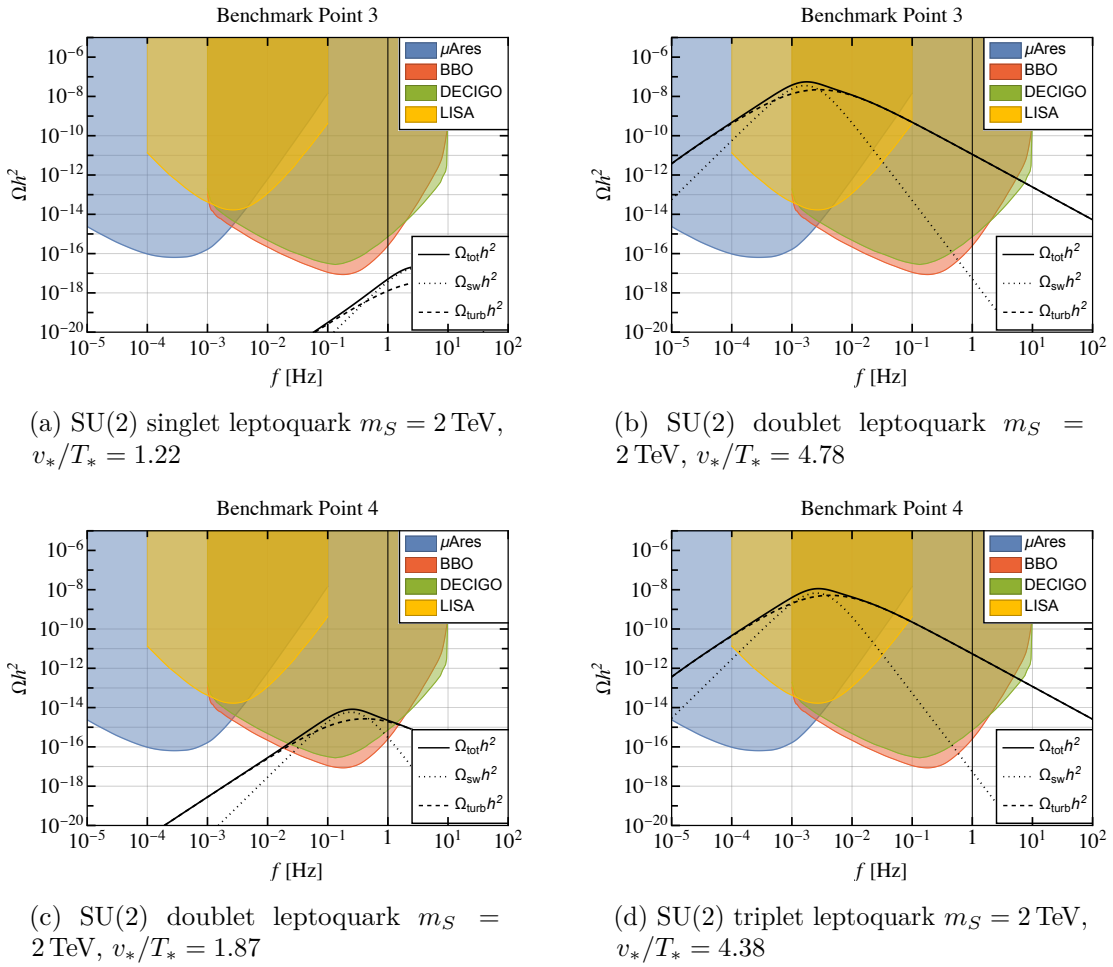


**Figure 3.** Gravitational wave signals for benchmark cases with 2 TeV leptiquarks. See the text for further discussion and explanation.

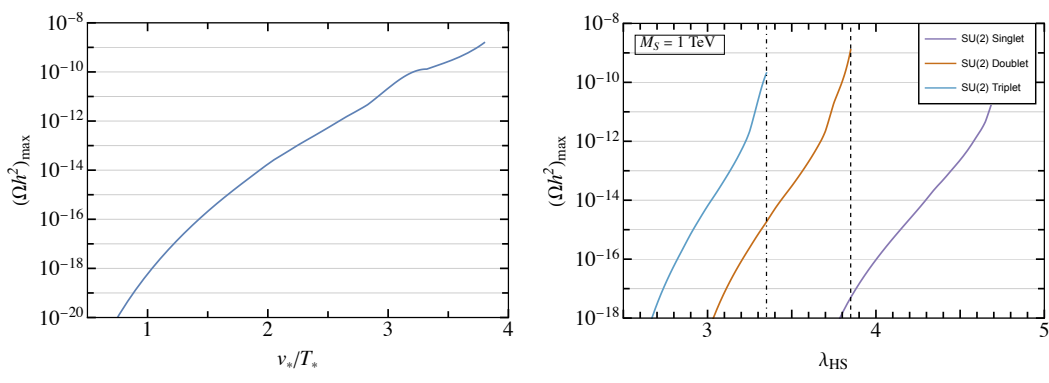


**Figure 4.** Left panel: maximal strength of the gravitational wave produced as a function of transition strength  $v_*/T_*$ . Right panel: maximal strength of gravitational wave produced by first-order EWPT induced by different type of leptiquarks of 1 TeV as a function of the Higgs portal coupling  $\lambda_{HS}$ . See the text for further discussion and explanation.

that for the same coupling, the first-order EWPT induced by the  $SU(2)$  multiplet with a higher dimension produces stronger gravitational waves. We also mark out the two benchmark values of the portal coupling in the right panel of figure 4 as the vertical lines. Supposing that the Higgs portal is measured to be in the region where first-order phase transition appears by future collider experiments, the gravitational waves detection provides an alternative method to further test the Higgs portal as well as determine the  $SU(2)$  representation of leptoquarks.

## 4 Conclusion

In this paper, we have explored the possibility that first-order EWPT induced by the coupling between a scalar leptoquark and the SM Higgs boson produces detectable gravitational wave signals. We have considered different  $SU(2)$  representations of the scalar leptoquark, including singlet, doublet and triplet. Despite the lack of VEV for leptoquark itself, a first-order EWPT can be induced due to the 1-loop order effects. In general, with first-order EWPTs, gravitational waves can be produced by multiple processes in the dynamical evolution of the scalar bubbles. The resulting gravitational waves form a stochastic background that can be probed by gravitational wave detectors.

We have calculated the effective potential of the SM Higgs field in the presence of a scalar leptoquark, including tree level and 1-loop level contributions as well as the resummation over the ring/daisy diagrams. By applying the conditions for first-order EWPT, we have found that the leptoquark can induce a first-order EWPT in the parameter space allowed by collider constraints and can be tested by future Higgs precision experiments. Enhanced by the internal degree of freedom of the particular leptoquark, we found that the leptoquark in the  $SU(2)$  representation with a higher dimension requires smaller coupling in order to trigger a first-order EWPT.

We have followed the standard procedure to compute the gravitational wave spectrum during first-order EWPTs. It turns out that the gravitational wave spectrum is mainly determined by the strength of the phase transition characterised by the ratio of the non-zero VEV and the temperature at the time that the transition happens. However, due to the difference in internal degrees of freedom, the strengths of first-order EWPTs induced by leptoquarks with the same masses and Higgs portal couplings but different  $SU(2)$  nature are different. Since the gravitational wave signals differ, this provides a possibility to determine the  $SU(2)$  representation of the leptoquarks through the observations of gravitational wave in particular regions of parameter space.

## Acknowledgments

BF acknowledges the Chinese Scholarship Council (CSC) Grant No. 201809210011 under agreements [2018]3101 and [2019]536. SFK acknowledges the STFC Consolidated Grant ST/L000296/1 and the European Union's Horizon 2020 Research and Innovation programme under Marie Skłodowska-Curie grant agreement HIDDeN European ITN project (H2020-MSCA-ITN-2019//860881-HIDDeN).

## A Production of gravitational waves during a first-order phase transition

As a beginning to discuss the phase transition dynamics, we need to determine the percolation temperature  $T_*$ . We use the condition derived in [80] to determine the percolation temperature, which is

$$I(T) \equiv \frac{4\pi}{3} \int_T^{T_c} \frac{\Gamma(T')}{T'^4 \mathcal{H}(T')} \left( \int_T^{T'} \frac{dT''}{\mathcal{H}(T'')} \right)^3 dT' = 0.34. \quad (\text{A.1})$$

The bubble nucleation rate  $\Gamma$  is given by [81]

$$\Gamma(T) = T^4 \left( \frac{S_E}{2\pi} \right)^{3/2} e^{-S_E}, \quad (\text{A.2})$$

where  $S_E$  is the Euclidean action. At finite temperature, the four-dimensional euclidean action  $S_E$  can be directly related to the three-dimensional Euclidean action  $S_3$  by the relation  $S_E = S_3/T$ . With the  $O(3)$  symmetry at high temperature,  $S_3$  is defined as

$$S_3 = 4\pi \int_0^\infty s^2 \left[ \frac{1}{2} \left( \frac{dh}{ds} \right)^2 + V_{\text{eff}}(h) \right] ds. \quad (\text{A.3})$$

By solving the corresponding Euclidean equation of motion

$$\frac{d^2 h}{ds^2} + \frac{2}{s} \frac{dh}{ds} - \frac{dV_{\text{eff}}}{dh} = 0 \quad (\text{A.4})$$

with boundary conditions

$$\left. \frac{dh}{ds} \right|_{s=0} = 0, \quad \text{and} \quad \lim_{s \rightarrow \infty} h(s) = 0, \quad (\text{A.5})$$

one can obtain the Euclidean action as a function of the temperature.

Given  $T_*$  and  $S_E$ , the inverse phase transition duration can be expressed as

$$\frac{\beta}{\mathcal{H}_*} = T \left. \frac{dS_E(T)}{dT} \right|_{T=T_*}, \quad (\text{A.6})$$

where  $\mathcal{H}_*$  is the Hubble parameter at  $T_*$ . The phase transition strength  $\alpha$  is the ratio of the difference in the trace anomaly  $\theta$  to the radiation energy density at the transition temperature, i.e.  $\alpha_{T_*} = \Delta\theta(T_*)/\rho(T_*)$ . The difference in the trace anomaly is given by

$$\Delta\theta(T) = -\Delta V + \frac{T}{4} \frac{d}{dT} \Delta V, \quad \Delta V = V_{\text{eff}}^\emptyset(T) - V_{\text{eff}}(0, T) \quad (\text{A.7})$$

with  $V_{\text{eff}}^\emptyset(T)$  the effective potential at the non-zero minimum. In the thin-shell limit, the contributions to the GW spectrum from different sources are given by [81]

$$\Omega_{\text{coll}}(f) = 2.30 \times 10^{-3} (R_* \mathcal{H}_*)^2 \left( \frac{\kappa_{\text{coll}} \alpha_{T_*}}{1 + \alpha_{T_*}} \right)^2 S_{\text{coll}}(f), \quad (\text{A.8a})$$

$$\Omega_{\text{sw}}(f) = 0.384 (\tau_{\text{sw}} \mathcal{H}_*) (R_* \mathcal{H}_*) \left( \frac{\kappa_{\text{sw}} \alpha_{T_*}}{1 + \alpha_{T_*}} \right)^2 S_{\text{sw}}(f), \quad (\text{A.8b})$$

$$\Omega_{\text{turb}}(f) = 6.85 (1 - \tau_{\text{sw}} \mathcal{H}_*) (R_* \mathcal{H}_*) \left( \frac{\kappa_{\text{sw}} \alpha_{T_*}}{1 + \alpha_{T_*}} \right)^{\frac{3}{2}} S_{\text{turb}}(f). \quad (\text{A.8c})$$

where  $R_*$  is the average bubble radius that can be estimated by [38]

$$R_* \mathcal{H}_* \simeq (8\pi)^{1/3} \text{Max}(v_w, c_s) \frac{\mathcal{H}_*}{\beta}. \quad (\text{A.9})$$

$c_s$  is the sound speed in the plasma and  $v_w$  is the wall speed that can be estimated analytically as [82, 83]

$$v_w \simeq \begin{cases} \sqrt{\frac{\Delta V}{\Delta \theta}}, & \sqrt{\frac{\Delta V}{\Delta \theta}} < v_J, \\ 1, & \sqrt{\frac{\Delta V}{\Delta \theta}} > v_J, \end{cases} \quad v_J = \frac{1}{\sqrt{3}} \frac{1 + \sqrt{3\alpha^2 + 2\alpha}}{1 + \alpha}. \quad (\text{A.10})$$

$\kappa_{\text{coll}}$ ,  $\kappa_{\text{sw}}$  and  $\kappa_t$  are the efficiency factors characterising the energy conversion during the phase transition. The efficiency factor for bubble collision is defined as the ratio of the bubble wall energy and the total released energy, i.e.  $\kappa_{\text{coll}} = E_{\text{wall}}/E_V$

$$\kappa_{\text{coll}} = \begin{cases} \left[ 1 - \frac{1}{3} \left( \frac{\tilde{\gamma}_*}{\gamma_{\text{eq}}} \right)^2 \right] \left( 1 - \frac{\alpha_\infty}{\alpha} \right), & \tilde{\gamma}_* < \gamma_{\text{eq}}, \\ \frac{2}{3} \frac{\tilde{\gamma}_*}{\gamma_{\text{eq}}} \left( 1 - \frac{\alpha_\infty}{\alpha} \right), & \tilde{\gamma}_* > \gamma_{\text{eq}}, \end{cases} \quad (\text{A.11})$$

where  $\gamma_{\text{eq}}$  is the bubble wall Lorentz factor when the bubble is in equilibrium and  $\tilde{\gamma}_*$  is the bubble wall Lorentz factor for a bubble with radius  $R_*$ .  $\alpha_\infty$  is defined as the ratio of the contribution from  $1 \rightarrow 1$  transitions to the pressure difference to the radiation energy density. For more details see [81, 84]. The efficiency factor for GW production from sound waves is given by

$$\kappa_{\text{sw}} = \frac{\alpha_{\text{eff}}}{\alpha} \frac{\alpha_{\text{eff}}}{0.73 + 0.083\sqrt{\alpha_{\text{eff}}} + \alpha_{\text{eff}}} \quad \text{with} \quad \alpha_{\text{eff}} = \alpha(1 - \kappa_{\text{coll}}). \quad (\text{A.12})$$

The parameter  $\tau_{\text{sw}}$  stands for the time when the sound wave period ends, after which the energy fluid motion is transferred to turbulence, with the expression [85]

$$\tau_{\text{sw}} = \frac{R_*}{U_f}, \quad U_f = \sqrt{\frac{3}{4} \frac{\alpha_{\text{eff}}}{1 + \alpha_{\text{eff}}} \kappa_{\text{sw}}}, \quad (\text{A.13})$$

where  $U_f$  is the root-mean-square fluid velocity.

The spectral form functions  $S_{\text{coll}}$ ,  $S_{\text{sw}}$  and  $S_{\text{turb}}$  read [81]

$$S_{\text{coll}}(f) = \left[ 1 + 0.05 \left( \frac{f}{f_{\text{coll}}} \right)^{-1.61} \right] \left( \frac{f}{f_{\text{coll}}} \right)^{2.54} \left[ 1 + 1.13 \left( \frac{f}{f_{\text{coll}}} \right)^{2.08} \right]^{-2.30}, \quad (\text{A.14a})$$

$$S_{\text{sw}}(f) = \left( \frac{f}{f_{\text{sw}}} \right)^3 \left( 1 + \frac{3}{4} \frac{f^2}{f_{\text{sw}}^2} \right)^{-\frac{7}{2}}, \quad (\text{A.14b})$$

$$S_{\text{turb}}(f) = \left( \frac{f}{f_{\text{turb}}} \right)^3 \left( 1 + \frac{f}{f_{\text{turb}}} \right)^{-\frac{11}{3}} \left( 1 + 8\pi \frac{f}{\mathcal{H}_*} \right)^{-1}. \quad (\text{A.14c})$$

The peak frequencies  $f_{\text{coll}}$ ,  $f_{\text{sw}}$  and  $f_{\text{turb}}$  are given by

$$f_{\text{coll}} = 16.5 \mu\text{Hz} \frac{0.62}{1.8 + 0.1v_w + v_w^2} \left( \frac{\beta}{\mathcal{H}_*} \right) \left( \frac{T_*}{100 \text{ GeV}} \right) \left( \frac{g_*}{100} \right)^{\frac{1}{6}}, \quad (\text{A.15a})$$

$$f_{\text{sw}} = 19 \mu\text{Hz} \frac{1}{v_w} \left( \frac{\beta}{\mathcal{H}_*} \right) \left( \frac{T_*}{100 \text{ GeV}} \right) \left( \frac{g_*}{100} \right)^{\frac{1}{6}}, \quad (\text{A.15b})$$

$$f_{\text{turb}} = 27 \mu\text{Hz} \frac{1}{v_w} \left( \frac{\beta}{\mathcal{H}_*} \right) \left( \frac{T_*}{100 \text{ GeV}} \right) \left( \frac{g_*}{100} \right)^{\frac{1}{6}}. \quad (\text{A.15c})$$

## References

- [1] J.C. Pati and A. Salam, *Unified Lepton-Hadron Symmetry and a Gauge Theory of the Basic Interactions*, *Phys. Rev. D* **8** (1973) 1240 [INSPIRE].
- [2] J.C. Pati and A. Salam, *Lepton Number as the Fourth Color*, *Phys. Rev. D* **10** (1974) 275 [INSPIRE].
- [3] G. Senjanovic and A. Sokorac, *Light Leptoquarks in SO(10)*, *Z. Phys. C* **20** (1983) 255 [INSPIRE].
- [4] W. Buchmuller and D. Wyler, *Constraints on SU(5) Type Leptoquarks*, *Phys. Lett. B* **177** (1986) 377 [INSPIRE].
- [5] P.H. Frampton, *Light leptoquarks as possible signature of strong electroweak unification*, *Mod. Phys. Lett. A* **7** (1992) 559 [INSPIRE].
- [6] S.S. Gershtein, A.A. Likhoded and A.I. Onishchenko, *TeV-scale leptoquarks from GUTs/string/M-theory unification*, *Phys. Rept.* **320** (1999) 159 [INSPIRE].
- [7] J. Fuentes-Martin, G. Isidori, J. Pagès and B.A. Stefanek, *Flavor non-universal Pati-Salam unification and neutrino masses*, *Phys. Lett. B* **820** (2021) 136484 [arXiv:2012.10492] [INSPIRE].
- [8] S.F. King, *Twin Pati-Salam theory of flavour with a TeV scale vector leptoquark*, *JHEP* **11** (2021) 161 [arXiv:2106.03876] [INSPIRE].
- [9] M. Fernández Navarro and S.F. King, *B-anomalies in a twin Pati-Salam theory of flavour including the 2022 LHCb  $R_{K^{(*)}}$  analysis*, *JHEP* **02** (2023) 188 [arXiv:2209.00276] [INSPIRE].
- [10] LHCb collaboration, *Search for lepton-universality violation in  $B^+ \rightarrow K^+ \ell^+ \ell^-$  decays*, *Phys. Rev. Lett.* **122** (2019) 191801 [arXiv:1903.09252] [INSPIRE].
- [11] BELLE collaboration, *Measurement of  $\mathcal{R}(D)$  and  $\mathcal{R}(D^*)$  with a semileptonic tagging method*, *Phys. Rev. Lett.* **124** (2020) 161803 [arXiv:1910.05864] [INSPIRE].
- [12] LHCb collaboration, *Test of lepton universality in beauty-quark decays*, *Nature Phys.* **18** (2022) 277 [arXiv:2103.11769] [INSPIRE].
- [13] LHCb collaboration, *Tests of lepton universality using  $B^0 \rightarrow K_S^0 \ell^+ \ell^-$  and  $B^+ \rightarrow K^{*+} \ell^+ \ell^-$  decays*, *Phys. Rev. Lett.* **128** (2022) 191802 [arXiv:2110.09501] [INSPIRE].
- [14] A. Angelescu et al., *Single leptoquark solutions to the B-physics anomalies*, *Phys. Rev. D* **104** (2021) 055017 [arXiv:2103.12504] [INSPIRE].
- [15] D. Bečirević et al., *Model with two scalar leptoquarks:  $R2$  and  $S3$* , *Phys. Rev. D* **106** (2022) 075023 [arXiv:2206.09717] [INSPIRE].
- [16] K.-M. Cheung, *Muon anomalous magnetic moment and leptoquark solutions*, *Phys. Rev. D* **64** (2001) 033001 [hep-ph/0102238] [INSPIRE].
- [17] E. Coluccio Leskow, G. D’Ambrosio, A. Crivellin and D. Müller,  *$(g-2)\mu$ , lepton flavor violation, and Z decays with leptoquarks: Correlations and future prospects*, *Phys. Rev. D* **95** (2017) 055018 [arXiv:1612.06858] [INSPIRE].

- [18] A. Crivellin, D. Müller and F. Saturnino, *Flavor Phenomenology of the Leptoquark Singlet-Triplet Model*, *JHEP* **06** (2020) 020 [[arXiv:1912.04224](#)] [[INSPIRE](#)].
- [19] P. Athron et al., *New physics explanations of  $a_\mu$  in light of the FNAL muon  $g - 2$  measurement*, *JHEP* **09** (2021) 080 [[arXiv:2104.03691](#)] [[INSPIRE](#)].
- [20] M. Du, J. Liang, Z. Liu and V.Q. Tran, *A vector leptoquark interpretation of the muon  $g - 2$  and  $B$  anomalies*, [arXiv:2104.05685](#) [[INSPIRE](#)].
- [21] S.-L. Chen, W.-W. Jiang and Z.-K. Liu, *Combined explanations of  $B$ -physics anomalies,  $(g - 2)_{e,\mu}$  and neutrino masses by scalar leptoquarks*, *Eur. Phys. J. C* **82** (2022) 959 [[arXiv:2205.15794](#)] [[INSPIRE](#)].
- [22] U. Mahanta, *Neutrino masses and mixing angles from leptoquark interactions*, *Phys. Rev. D* **62** (2000) 073009 [[hep-ph/9909518](#)] [[INSPIRE](#)].
- [23] F.F. Deppisch, S. Kulkarni, H. Päs and E. Schumacher, *Leptoquark patterns unifying neutrino masses, flavor anomalies, and the diphoton excess*, *Phys. Rev. D* **94** (2016) 013003 [[arXiv:1603.07672](#)] [[INSPIRE](#)].
- [24] O. Popov and G.A. White, *One Leptoquark to unify them? Neutrino masses and unification in the light of  $(g - 2)_\mu$ ,  $R_{D^{(*)}}$  and  $R_K$  anomalies*, *Nucl. Phys. B* **923** (2017) 324 [[arXiv:1611.04566](#)] [[INSPIRE](#)].
- [25] Y. Cai, J. Gargalionis, M.A. Schmidt and R.R. Volkas, *Reconsidering the One Leptoquark solution: flavor anomalies and neutrino mass*, *JHEP* **10** (2017) 047 [[arXiv:1704.05849](#)] [[INSPIRE](#)].
- [26] P.S. Bhupal Dev, R. Mohanta, S. Patra and S. Sahoo, *Unified explanation of flavor anomalies, radiative neutrino masses, and ANITA anomalous events in a vector leptoquark model*, *Phys. Rev. D* **102** (2020) 095012 [[arXiv:2004.09464](#)] [[INSPIRE](#)].
- [27] A. Crivellin, D. Müller and F. Saturnino, *Leptoquarks in oblique corrections and Higgs signal strength: status and prospects*, *JHEP* **11** (2020) 094 [[arXiv:2006.10758](#)] [[INSPIRE](#)].
- [28] A. D’Alise et al., *Standard model anomalies: lepton flavour non-universality,  $g - 2$  and  $W$ -mass*, *JHEP* **08** (2022) 125 [[arXiv:2204.03686](#)] [[INSPIRE](#)].
- [29] P. Athron et al., *Hadronic uncertainties versus new physics for the  $W$  boson mass and Muon  $g - 2$  anomalies*, *Nature Commun.* **14** (2023) 659 [[arXiv:2204.03996](#)] [[INSPIRE](#)].
- [30] K. Cheung, W.-Y. Keung and P.-Y. Tseng, *Isodoublet vector leptoquark solution to the muon  $g - 2$ ,  $R_{K,K^*}$ ,  $R_{D,D^*}$ , and  $W$ -mass anomalies*, *Phys. Rev. D* **106** (2022) 015029 [[arXiv:2204.05942](#)] [[INSPIRE](#)].
- [31] A. Bhaskar, A.A. Madathil, T. Mandal and S. Mitra, *Combined explanation of  $W$ -mass, muon  $g - 2$ ,  $R_{K^{(*)}}$  and  $R_{D^{(*)}}$  anomalies in a singlet-triplet scalar leptoquark model*, *Phys. Rev. D* **106** (2022) 115009 [[arXiv:2204.09031](#)] [[INSPIRE](#)].
- [32] S.-P. He, *Leptoquark and vector-like quark extended model for simultaneous explanation of  $W$  boson mass and muon  $g - 2$  anomalies*, *Chin. Phys. C* **47** (2023) 043102 [[arXiv:2205.02088](#)] [[INSPIRE](#)].
- [33] S. Kolb, M. Hirsch and H.V. Klapdor-Kleingrothaus, *Bounds on leptoquark parameters with nonvanishing leptoquark Higgs couplings*, *Phys. Lett. B* **391** (1997) 131 [[INSPIRE](#)].
- [34] I. Doršner et al., *Physics of leptoquarks in precision experiments and at particle colliders*, *Phys. Rept.* **641** (2016) 1 [[arXiv:1603.04993](#)] [[INSPIRE](#)].
- [35] D. Curtin, P. Meade and C.-T. Yu, *Testing Electroweak Baryogenesis with Future Colliders*, *JHEP* **11** (2014) 127 [[arXiv:1409.0005](#)] [[INSPIRE](#)].
- [36] C. Caprini et al., *Science with the space-based interferometer eLISA. II: Gravitational waves from cosmological phase transitions*, *JCAP* **04** (2016) 001 [[arXiv:1512.06239](#)] [[INSPIRE](#)].



- [37] D.J. Weir, *Gravitational waves from a first order electroweak phase transition: a brief review*, *Phil. Trans. Roy. Soc. Lond. A* **376** (2018) 20170126 [[arXiv:1705.01783](#)] [[INSPIRE](#)].
- [38] C. Caprini et al., *Detecting gravitational waves from cosmological phase transitions with LISA: an update*, *JCAP* **03** (2020) 024 [[arXiv:1910.13125](#)] [[INSPIRE](#)].
- [39] A. Beniwal et al., *Gravitational wave, collider and dark matter signals from a scalar singlet electroweak baryogenesis*, *JHEP* **08** (2017) 108 [[arXiv:1702.06124](#)] [[INSPIRE](#)].
- [40] P. Di Bari, D. Marfatia and Y.-L. Zhou, *Gravitational waves from first-order phase transitions in Majoron models of neutrino mass*, *JHEP* **10** (2021) 193 [[arXiv:2106.00025](#)] [[INSPIRE](#)].
- [41] L. Bian, Y.-L. Tang and R. Zhou, *FIMP dark matter mediated by a massive gauge boson around the phase transition period and the gravitational waves production*, *Phys. Rev. D* **106** (2022) 035028 [[arXiv:2111.10608](#)] [[INSPIRE](#)].
- [42] S. Demidov, D. Gorbunov and E. Kriukova, *Gravitational waves from first-order electroweak phase transition in a model with light sgoldstinos*, *JHEP* **07** (2022) 061 [[arXiv:2112.06083](#)] [[INSPIRE](#)].
- [43] L. Gráf, S. Jana, A. Kaladharan and S. Saad, *Gravitational wave imprints of left-right symmetric model with minimal Higgs sector*, *JCAP* **05** (2022) 003 [[arXiv:2112.12041](#)] [[INSPIRE](#)].
- [44] R. Zhou, L. Bian and Y. Du, *Electroweak phase transition and gravitational waves in the type-II seesaw model*, *JHEP* **08** (2022) 205 [[arXiv:2203.01561](#)] [[INSPIRE](#)].
- [45] T.-K. Chen, C.-W. Chiang, C.-T. Huang and B.-Q. Lu, *Updated constraints on the Georgi-Machacek model and its electroweak phase transition and associated gravitational waves*, *Phys. Rev. D* **106** (2022) 055019 [[arXiv:2205.02064](#)] [[INSPIRE](#)].
- [46] B.-Q. Lu, C.-W. Chiang and D. Huang, *Probing WIMPs in space-based gravitational wave experiments*, *Phys. Lett. B* **833** (2022) 137308 [[arXiv:2205.08380](#)] [[INSPIRE](#)].
- [47] A. Dasgupta, P.S.B. Dev, A. Ghoshal and A. Mazumdar, *Gravitational wave pathway to testable leptogenesis*, *Phys. Rev. D* **106** (2022) 075027 [[arXiv:2206.07032](#)] [[INSPIRE](#)].
- [48] L. Niemi, P. Schicho and T.V.I. Tenkanen, *Singlet-assisted electroweak phase transition at two loops*, *Phys. Rev. D* **103** (2021) 115035 [[arXiv:2103.07467](#)] [[INSPIRE](#)].
- [49] P. Schicho, T.V.I. Tenkanen and G. White, *Combining thermal resummation and gauge invariance for electroweak phase transition*, *JHEP* **11** (2022) 047 [[arXiv:2203.04284](#)] [[INSPIRE](#)].
- [50] M. Quiros, *Finite temperature field theory and phase transitions*, in the proceedings of the *ICTP Summer School in High-Energy Physics and Cosmology*, (1999), p. 187–259 [[hep-ph/9901312](#)] [[INSPIRE](#)].
- [51] A.D. Linde, *Infrared Problem in Thermodynamics of the Yang-Mills Gas*, *Phys. Lett. B* **96** (1980) 289 [[INSPIRE](#)].
- [52] D. Croon et al., *Theoretical uncertainties for cosmological first-order phase transitions*, *JHEP* **04** (2021) 055 [[arXiv:2009.10080](#)] [[INSPIRE](#)].
- [53] R.R. Parwani, *Resummation in a hot scalar field theory*, *Phys. Rev. D* **45** (1992) 4695 [Erratum *ibid.* **48** (1993) 5965] [[hep-ph/9204216](#)] [[INSPIRE](#)].
- [54] D. Curtin, P. Meade and H. Ramani, *Thermal Resummation and Phase Transitions*, *Eur. Phys. J. C* **78** (2018) 787 [[arXiv:1612.00466](#)] [[INSPIRE](#)].
- [55] P.B. Arnold and O. Espinosa, *The Effective potential and first order phase transitions: Beyond leading-order*, *Phys. Rev. D* **47** (1993) 3546 [Erratum *ibid.* **50** (1994) 6662] [[hep-ph/9212235](#)] [[INSPIRE](#)].
- [56] J.M. Cline, K. Kainulainen and M. Trott, *Electroweak Baryogenesis in Two Higgs Doublet Models and B meson anomalies*, *JHEP* **11** (2011) 089 [[arXiv:1107.3559](#)] [[INSPIRE](#)].

- [57] G. Hiller and I. Nisandzic,  $R_K$  and  $R_{K^*}$  beyond the standard model, *Phys. Rev. D* **96** (2017) 035003 [[arXiv:1704.05444](#)] [[INSPIRE](#)].
- [58] E.J. Weinberg and A.-Q. Wu, Understanding complex perturbative effective potentials, *Phys. Rev. D* **36** (1987) 2474 [[INSPIRE](#)].
- [59] ATLAS collaboration, Measurements of the Higgs boson production and decay rates and constraints on its couplings from a combined ATLAS and CMS analysis of the LHC pp collision data at  $\sqrt{s} = 7$  and 8 TeV, ATLAS-CONF-2015-044 (2015) [[INSPIRE](#)].
- [60] CMS collaboration, Measurements of the Higgs boson production and decay rates and constraints on its couplings from a combined ATLAS and CMS analysis of the LHC pp collision data at  $\sqrt{s} = 7$  and 8 TeV, CMS-PAS-HIG-15-002 (2015) [[INSPIRE](#)].
- [61] ATLAS collaboration, Measurement of the properties of Higgs boson production at  $\sqrt{s} = 13$  TeV in the  $H \rightarrow \gamma\gamma$  channel using  $139 \text{ fb}^{-1}$  of pp collision data with the ATLAS experiment, [arXiv:2207.00348](#) [[INSPIRE](#)].
- [62] CMS collaboration, A portrait of the Higgs boson by the CMS experiment ten years after the discovery, *Nature* **607** (2022) 60 [[arXiv:2207.00043](#)] [[INSPIRE](#)].
- [63] PARTICLE DATA GROUP collaboration, Review of Particle Physics, *PTEP* **2020** (2020) 083C01 [[INSPIRE](#)].
- [64] CMS collaboration, Sensitivity projections for Higgs boson properties measurements at the HL-LHC, CMS-PAS-FTR-18-011 (2018) [[INSPIRE](#)].
- [65] D. d'Enterria, Higgs physics at the Future Circular Collider, *PoS ICHEP2016* (2017) 434 [[arXiv:1701.02663](#)] [[INSPIRE](#)].
- [66] FCC collaboration, FCC-ee: The Lepton Collider: Future Circular Collider Conceptual Design Report Volume 2, *Eur. Phys. J. ST* **228** (2019) 261 [[INSPIRE](#)].
- [67] P. Bambade et al., The International Linear Collider: A Global Project, [arXiv:1903.01629](#) [[INSPIRE](#)].
- [68] F. An et al., Precision Higgs physics at the CEPC, *Chin. Phys. C* **43** (2019) 043002 [[arXiv:1810.09037](#)] [[INSPIRE](#)].
- [69] M. Ruan, Y. Fang, G. Li and D. Yu, CEPC Research Report: Higgs Physics Analysis, [arXiv:2107.09820](#) [[INSPIRE](#)].
- [70] A. Crivellin, C. Greub, D. Müller and F. Saturnino, Scalar Leptoquarks in Leptonic Processes, *JHEP* **02** (2021) 182 [[arXiv:2010.06593](#)] [[INSPIRE](#)].
- [71] M. Dine et al., Towards the theory of the electroweak phase transition, *Phys. Rev. D* **46** (1992) 550 [[hep-ph/9203203](#)] [[INSPIRE](#)].
- [72] CMS collaboration, Search for singly and pair-produced leptoquarks coupling to third-generation fermions in proton-proton collisions at  $\sqrt{s} = 13$  TeV, CMS-PAS-EXO-19-015 (2020) [[INSPIRE](#)].
- [73] CMS collaboration, Search for singly and pair-produced leptoquarks coupling to third-generation fermions in proton-proton collisions at  $\sqrt{s} = 13$  TeV, *Phys. Lett. B* **819** (2021) 136446 [[arXiv:2012.04178](#)] [[INSPIRE](#)].
- [74] ATLAS collaboration, Search for pair production of third-generation scalar leptoquarks decaying into a top quark and a  $\tau$ -lepton in pp collisions at  $\sqrt{s} = 13$  TeV with the ATLAS detector, *JHEP* **06** (2021) 179 [[arXiv:2101.11582](#)] [[INSPIRE](#)].
- [75] ATLAS collaboration, Search for scalar leptoquarks in the  $b\tau\tau$  final state in pp collisions at  $\sqrt{s} = 13$  TeV with the ATLAS detector, ATLAS-CONF-2022-037 (2022) [[INSPIRE](#)].
- [76] V. Corbin and N.J. Cornish, Detecting the cosmic gravitational wave background with the big bang observer, *Class. Quant. Grav.* **23** (2006) 2435 [[gr-qc/0512039](#)] [[INSPIRE](#)].

- [77] DECIGO WORKING GROUP collaboration, *Primordial gravitational wave and DECIGO*, *PoS KMI2019* (2019) 019 [[INSPIRE](#)].
- [78] S. Kawamura et al., *Current status of space gravitational wave antenna DECIGO and B-DECIGO*, *PTEP* **2021** (2021) 05A105 [[arXiv:2006.13545](#)] [[INSPIRE](#)].
- [79] A. Sesana et al., *Unveiling the gravitational universe at  $\mu$ -Hz frequencies*, *Exper. Astron.* **51** (2021) 1333 [[arXiv:1908.11391](#)] [[INSPIRE](#)].
- [80] J. Ellis, M. Lewicki and J.M. No, *On the Maximal Strength of a First-Order Electroweak Phase Transition and its Gravitational Wave Signal*, *JCAP* **04** (2019) 003 [[arXiv:1809.08242](#)] [[INSPIRE](#)].
- [81] J. Ellis, M. Lewicki and V. Vaskonen, *Updated predictions for gravitational waves produced in a strongly supercooled phase transition*, *JCAP* **11** (2020) 020 [[arXiv:2007.15586](#)] [[INSPIRE](#)].
- [82] J. Ellis et al., *The scalar singlet extension of the Standard Model: gravitational waves versus baryogenesis*, *JHEP* **01** (2023) 093 [[arXiv:2210.16305](#)] [[INSPIRE](#)].
- [83] M. Lewicki, M. Merchand and M. Zych, *Electroweak bubble wall expansion: gravitational waves and baryogenesis in Standard Model-like thermal plasma*, *JHEP* **02** (2022) 017 [[arXiv:2111.02393](#)] [[INSPIRE](#)].
- [84] J. Ellis, M. Lewicki, J.M. No and V. Vaskonen, *Gravitational wave energy budget in strongly supercooled phase transitions*, *JCAP* **06** (2019) 024 [[arXiv:1903.09642](#)] [[INSPIRE](#)].
- [85] J. Ellis, M. Lewicki and J.M. No, *Gravitational waves from first-order cosmological phase transitions: lifetime of the sound wave source*, *JCAP* **07** (2020) 050 [[arXiv:2003.07360](#)] [[INSPIRE](#)].